RADIATION RESEARCH **159**, 154–160 (2003)
0033-7587/03 $5.00

High-Energy Neutron Spectroscopy with Thick Silicon Detectors

James D. Kinnison,[a,1] Richard H. Maurer,[a] David R. Roth[a] and Robert C. Haight[b]

[a] *The Johns Hopkins University Applied Physics Laboratory, Laurel, Maryland; and* [b] *Los Alamos Neutron Science Center, Los Alamos, New Mexico*

Kinnison, J. D., Maurer, R. H., Roth, D. R. and Haight, R. C. High-Energy Neutron Spectroscopy with Thick Silicon Detectors. *Radiat. Res.* 159, 154–160 (2003).

The high-energy neutron component of the space radiation environment in thick structures such as the International Space Station contributes to the total radiation dose received by an astronaut. Detector design constraints such as size and mass have limited the energy range of neutron spectrum measurements in orbit to about 12 MeV in Space Shuttle studies. We present a new method for high-energy neutron spectroscopy using small silicon detectors that can extend these measurements to more than 500 MeV. The methodology is based on measurement of the detector response function for high-energy neutrons and inversion of this response function with measured deposition data to deduce neutron energy spectra. We also present the results of an initial shielding study performed with the thick silicon detector system for high-energy neutrons incident on polyethylene.

INTRODUCTION

High-energy charged particles of extra-galactic, galactic and solar origin collide with spacecraft structures in Earth orbit outside the atmosphere and in interplanetary travel beyond the Earth's magnetosphere. These primaries create a number of secondary particles inside the structures that can produce a significant ionizing radiation environment. The primary high-energy cosmic rays and trapped or solar protons collide with common spacecraft materials such as aluminum, silicon and graphite epoxy, creating secondaries that are mostly charged-particle fragments, protons, α particles and neutrons. Charged particles are readily detected; however, neutrons, being electrically neutral, are more difficult to detect and monitor. These neutrons are reported to contribute 30–60% of the dose inside space structures. A recent measurement of low-energy neutrons (less than 10 MeV) on a shuttle flight indicates a contribution of 36% in a shuttle locker (*1*). Correlation of recent neutron dosimetry data from high-altitude aircraft flights (40,000–60,000 ft.) with neutron fluences below 10 MeV indicates that there are at least as many neutrons above as below 10 MeV (*2*). This high-energy component is presently not measured by most detectors in space.

The high-energy neutron component is important in accurately assessing the radiation threat to long-term inhabitants or travelers for space missions such as the months of occupation of the International Space Station or the years required for the baseline mission to Mars. A complete risk assessment includes the increased probability for carcinogenesis, DNA and central nervous system damage—some of which may be caused by a single hit of an energetic ion or neutron. With respect to cancer, astronauts on these long missions will be bombarded by high-energy neutrons that can penetrate and be moderated by body tissue, eventually reacting and producing damage in interior organs such as the liver or spleen. Measurements of the high-energy neutron component of the large-structure radiation environment are needed to comprehensively assess astronaut risk and to design mitigation strategies.

Silicon detectors are commonly used for charged-particle detection. Electromagnetic interactions of a charged particle incident on the detector material efficiently remove electrons from target atoms and provide large electrical signals in the detector. Neutrons, being uncharged, do not directly ionize target atoms and so do not themselves produce charge in a detector. Neutrons can be detected indirectly in silicon detectors by elastic and inelastic reactions with the silicon nuclei that produce secondary charged particles. In a mixed charged-particle and neutron environment such as is found inside thick spacecraft structures, a combination of a silicon detector and an anti-coincidence shield such as a CsI scintillator can be used to measure neutron energy and charged-particle deposition spectra simultaneously.

Nuclear reactions have smaller cross sections than electromagnetic interactions, and the efficiency of a silicon-based neutron detector is correspondingly lower than that for charged-particle detection, by as much as two orders of magnitude for high-energy neutrons. In general, the mean free path in a detector material grows as the incident neutron energy is increased so that for thin detectors the probability of an interaction—and also the detector efficiency—becomes unacceptably low. However, thick silicon detectors provide greater numbers of target nuclei for neutron interactions and also allow for more energy deposition from

[1] Address for correspondence: MS 23-270, Applied Physics Laboratory, 11100 Johns Hopkins Road, Laurel, MD 20723; e-mail: jim.kinnison@jhuapl.edu.

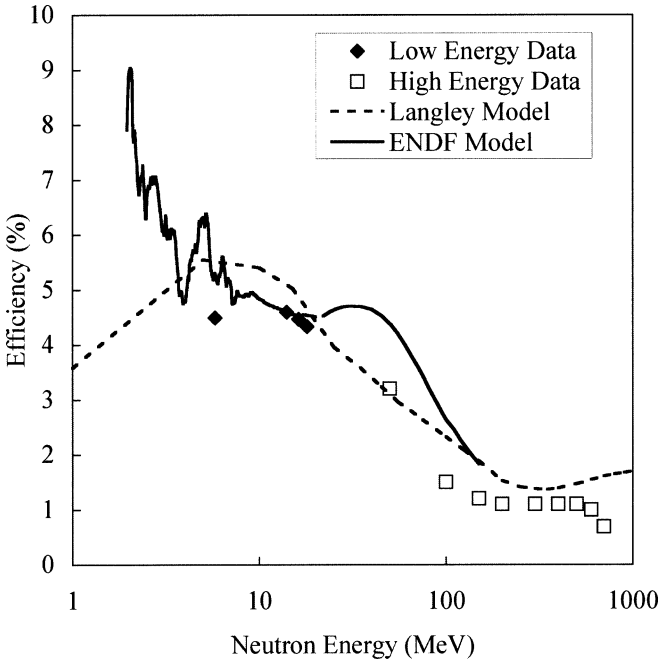

FIG. 1. Measured efficiency of a thick silicon detector compared with efficiency calculated using common models of the neutron–silicon reaction cross section. The detector is 2 cm² by 0.5-cm-thick cylinder irradiated on the front circular face.

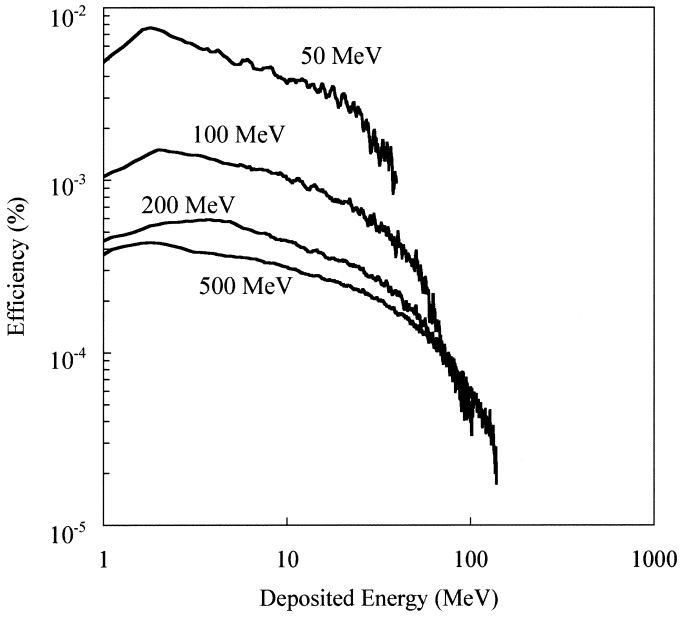

FIG. 2. Depositions from monoenergetic slices of the LANSCE neutron beam. Individual deposition curves correspond to single time-of-flight channels with narrow neutron energy width. These curves show that deposition spectra (and corresponding response functions) for different neutron energies are distinct, which indicates that the responses are suitable for use in the inversion process described in this work. Note that only a few curves are shown for clarity.

charged secondary particles. Figure 1 gives the measured efficiency of a cylindrical 2 cm² × 0.5-cm lithium-drifted silicon detector as a function of neutron energy as well as predicted efficiency based on several commonly used models of neutron–silicon interactions. Note that the measured efficiency is generally below the model predictions because only depositions above a 0.25 MeV noise cutoff were included, whereas the models consider all depositions (*3, 4*). Figure 1 indicates that for applications in which physical size and mass are important, such as spacecraft, thick silicon detectors can provide sufficient data to measure neutron spectra effectively. Deposited energy spectra for the same 0.5-cm detector from experiments at the Los Alamos Neutron Science Center (LANSCE), shown in Fig. 2, indicate that such a detector and associated electronics can collect up to about 150 MeV of deposited energy from charged secondaries and that the energy deposition spectra for different neutron energy ranges are distinct. These deposition spectra form the basis for unfolding incident neutron spectra from silicon detector data.

THEORY

Fundamental Interactions

Neutrons colliding with silicon nuclei undergo both elastic and nonelastic interactions. Elastic reactions are those in which the total kinetic energy and momentum of the neutron–nucleus system are conserved. In elastic collisions, the products are the same as the incident particles with the total kinetic energy shared according to two-body kinematics. The resultant silicon recoil nucleus is charged and deposits energy in the detector through ionization of the surrounding medium along its path. From the kinematics of elastic collisions, the maximum kinetic energy transferred to a silicon nucleus in this way is about 13% of the incident neutron energy (*5*).

Nonelastic reactions are those processes in which the product nucleus is different from the target nucleus or is left in an internal state different from the original target nucleus. For instance, the (n,α) reaction is $n + {}^{28}Si \rightarrow \alpha = {}^{25}Mg$. Both the α particle and the magnesium nucleus have initial kinetic energy that they then lose in the detector, and the total energy measured by the detector for the event is the sum of the energy lost by each fragment. In theory, the maximum total energy detected in a nonelastic interaction can be as high as the incident neutron energy plus any binding energy that may be released in the breakup of the target nucleus. In practice, energy deposition in the detector is limited by the size and shape of the detector. Long-range charged particles such as energetic protons may escape from the detector before they deposit all their energy in the detector.

Above about 250 MeV, neutrons can interact directly with nucleons in the silicon nucleus to form pions through reactions such as $n+p \rightarrow n+n+\pi^+$ or $n+n \rightarrow n+p+\pi^-$ (*6*). Charged pions lose energy through ionization and by reacting with additional silicon nuclei or decaying in about 10^{-8} s to form charged secondary particles that also deposit charge in the silicon. The result is an enhancement in the total cross section above the neutron energy threshold for pion formation to occur at approximately 260 MeV. Figure 3 shows the enhancement in silicon detector efficiency brought about by the increase in total interaction cross section. Here efficiency is counts per neutron in the detector for all depositions greater than 0.25 MeV.

Detector Response

A beam of monoenergetic neutrons produces a distribution of energy deposition events in a silicon detector, as shown previously in Fig. 2. When normalized by the beam fluence, this spectrum is a detector response function evaluated at the incident neutron energy and is given by

$$C(E_D) = A(E_D, E_N)\Phi(E_N)\delta E_N, \quad (1)$$

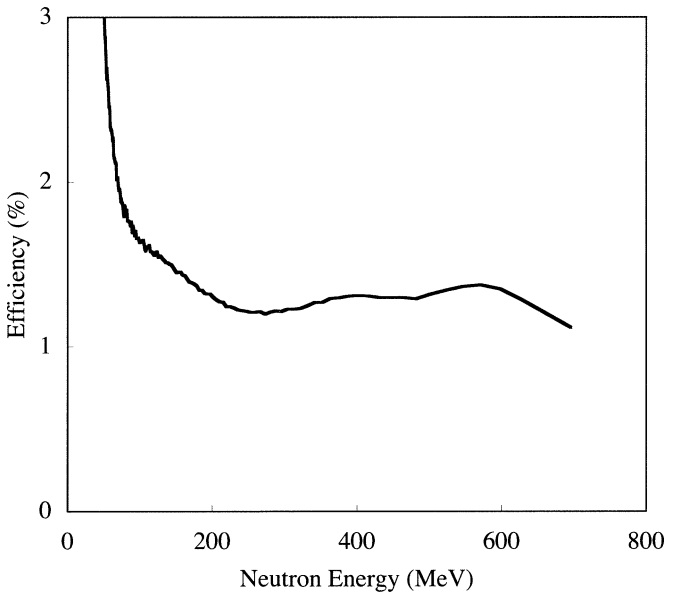

FIG. 3. Total efficiency in the silicon detector as a function of neutron energy. The increase in efficiency above 280 MeV represents the addition of charged pion generating reactions with a threshold of about 260 MeV.

where C is the number of counts detected at a given deposited energy E_D, $\Phi(E_N)\delta E_n$ is the integral neutron fluence centered at E_N, and A is the response function of the detector, which depends on both the incident and deposited energies. One can use this relationship to make an estimate of the neutron energy spectrum from a measured count spectrum through standard least-squares fitting of count data to Eq. (1). If the source spectrum is not monoenergetic Eq. (1) can be generalized as

$$C(E_D) = \int A(E_D, E_N)\Phi(E_N)\, dE_N. \tag{2}$$

Or in discrete form in both deposited energy and neutron energy,

$$C_i = \sum_j c_{ij} = \sum_j A_{ij}\Phi_j\Delta E_n, \tag{3}$$

where c_{ij} is the portion of total counts in the ith energy deposition bin generated by the jth neutron energy bin and A_{ij} is the response matrix element for the ith energy deposition bin and jth neutron energy bin. In matrix notation, this can be written as $C = A\Phi$.

If one measures the count spectrum with a detector for which the response matrix, A, is known, Eq. (3) becomes a system of linear equations which one can solve for estimates of the fluence in each neutron energy bin. In most experiments, the number of energy deposition bins is greater than the number of neutron fluence bins, so the system is overdetermined and can be solved through multiple regression techniques. In this work, we used a constrained linear least-squares algorithm implemented in MATLAB (*7*) which takes advantage of the positive-definite nature of the neutron fluence to invert Eq. (3) and give a neutron spectrum from count data.

EXPERIMENTS

Response Measurement

In August 2000, we carried out a series of experiments to measure the response matrix of a 0.5-cm silicon detector manufactured by EG&G ORTEC, now Perkin-Elmer (Model L-045-200-5). This device is a 2-cm^2 lithium-drifted detector with an α-particle resolution of 45 keV (FWHM) at 5.486 MeV. We integrated this detector and associated pulse-height analysis electronics into the time-of-flight spectrometer on the 90-m beamline at LANSCE as shown in Fig. 4.

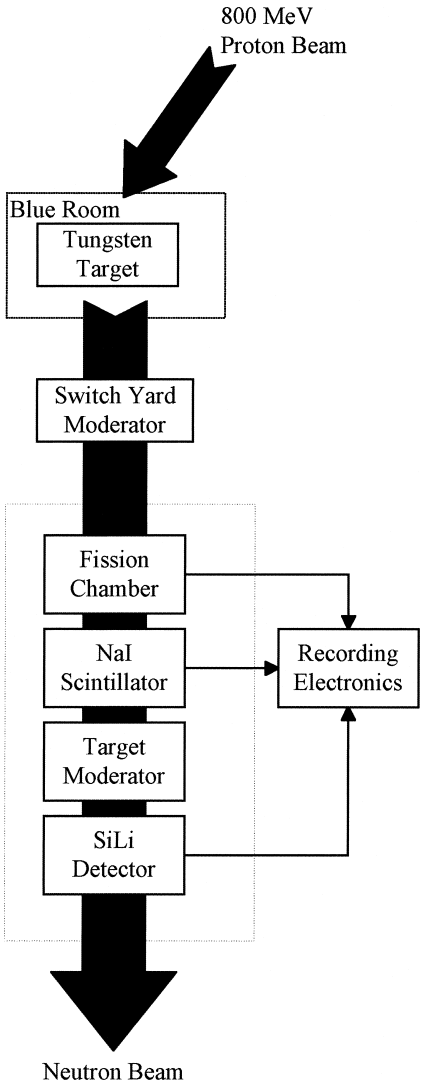

FIG. 4. LANSCE experiment configuration. The detector was approximately 90 m from the tungsten production target. The switchyard moderator was used for beam shaping to reduce low-energy neutron aliasing and to provide the unknown beam for validation experiments, while the moderator at the detector was used only for polyethylene shielding studies.

The LANSCE neutron beam is produced by a pulsed 800 MeV proton beam interacting with a 7.5-cm-long tungsten target (*8*). The broad-spectrum pulsed neutrons produced by this interaction are collimated into neutron beams with energy less than 1 MeV to a maximum energy of 800 MeV. Attenuating materials can be placed in the beam to change the shape of the neutron flux spectrum and, in particular, to reduce the number of low-energy neutrons. When a neutron interacts with our detector, the energy deposition is stored as well as the time of flight for the neutron from the tungsten production target to our detector. This time difference

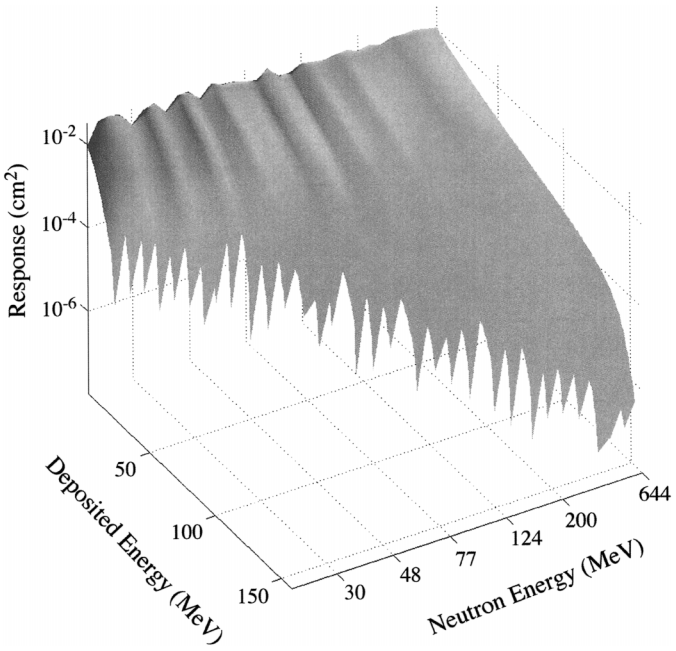

FIG. 5. Surface plot of response matrix as a function of incident neutron energy and deposited energy. The response is the number of events which deposit more than a given energy per unit neutron fluence and is a macroscopic cross section for the silicon detector.

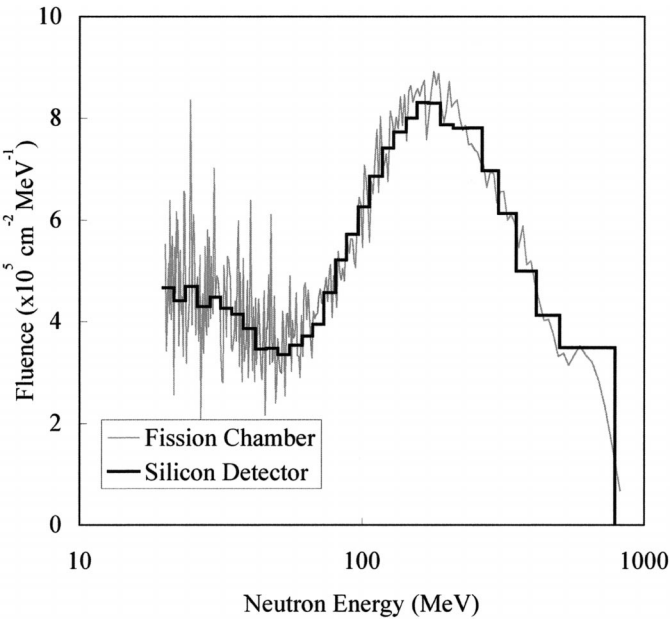

FIG. 6. Comparison of measured differential neutron fluence from the fission foil chamber and the silicon detector for the experiment in which the response function was measured. These data serve as a consistency check of the inversion process and the measured response function.

gives the energy of the neutron inducing the interaction. Therefore, we have simultaneously measured the incident neutron energy and energy deposited in the detector for each neutron–silicon interaction. In addition, the LANSCE uranium-238 foil fission chamber provided an independent measurement of the incident neutron spectrum (*9*). Since the time-of-flight channels are narrow, each is a nearly monoenergetic slice of the incident neutron spectrum. The energy deposition spectra normalized by the neutron fluence for a channel are the ''monoenergetic'' response matrix elements for the neutron energy corresponding to that time-of-flight channel; in these measurements, the fluence in each channel was determined by the fission chamber. Figure 5 gives the measured response matrix as used in subsequent neutron spectrum measurements with the silicon detector; the values of A_{ij} in Eq. (3) are shown here. Figure 6 gives the neutron spectrum for the experiment as measured by the fission chamber and as calculated from the overall count spectrum in the silicon detector through the inversion of Eq. (3) as a consistency check for the inversion process.

The low neutron energy limit of the response matrix is determined by the frequency of the initial proton pulse which generates the neutron beam. Neutrons with flight times greater than the spacing between proton pulses will masquerade as higher-energy neutrons in the next pulse; the switchyard moderator for these measurements was designed to remove neutrons with energy below about 20 MeV, the lower limit for this experiment. We have performed additional experiments at the Columbia University Radiological Research Accelerator Facility to extend the response matrix to neutron energies between 5 and 20 MeV; analysis of data from these experiments will be complete in 2002.

Experimental Error

In an experiment where C_i is measured and neutron fluences are calculated through the inversion process as described above, the uncertainty in the derived neutron fluences depends on two components—uncertainty in the count data, C_i, and error in the response function, A_{ij}. Neglecting any systematic error in the count data measurement, the error in the C_i's is given by Poisson statistics such that $\sigma_i^2 = C_i$.

The error in the response function is given by the following two components: systematic error in the experiment used to measure the response function and random error associated with each element of the response function matrix. The neutron source beam for the August 2000 experiments was pulsed, and the energy of the source neutrons was measured with a time-of-flight (TOF) spectrometer using the beam pulse as a timing marker. Low-energy neutrons from one pulse were detected in the TOF spectrometer in the subsequent pulse as a high-energy neutron; this is the primary source of systematic error in the response function measurement. The switchyard moderator shown in Fig. 4 reduced the low-energy component of the source beam so that the number of neutrons in a given time channel as a result of aliasing from a previous pulse is less than 1% of the total fluence in that channel. We neglect this systematic error in subsequent error analysis.

As discussed earlier, we determined the response matrix

by measuring energy deposition spectra simultaneously with neutron fluence for each neutron energy bin. The error in the response matrix elements depends on the error in the deposition spectra and in the neutron fluences and, by error propagation using the definition of the response matrix, can be written as

$$\sigma_{ij}^2 = (A_{ij}/\Psi_j) + e_j^2 A_{ij}^2, \quad (4)$$

where e_j is the relative error in the jth neutron energy bin as measured by the fission chamber. For our experiments, e_j was about 20%, which dominates the error in each response matrix element except for the last few data points in each energy deposition, spectrum where Poisson counting statistics dominate. When the error in each matrix element is small compared to the variation in each column of the matrix, bias introduced in the least-squares inversion process by ignoring the matrix element errors is small. This is indeed the case in our present work, and in future experiments, we will reduce e_j to below 5% by measuring the deposition spectra in longer exposures to further reduce the bias introduced by the matrix element error.

For an experiment in which the measurement errors of C are uncorrelated, estimated variances for the fluence estimates are given by the diagonal elements of the covariance matrix,

$$S^2 = (A^T W A)^{-1}, \quad (5)$$

where A^T is the transpose of the response matrix and W is a diagonal weight matrix whose elements are given by the uncertainties in the measured count data; i.e. $W_{ii} = 1/\sigma_i^2 = 1/C_i$. In all subsequent analyses, errors in derived neutron fluences are calculated using Eq. (5). In general, the uncertainty in neutron fluence for our experiments is 40–55%.

Validation

Subsequent to the initial experiment to measure the detector response function, an additional experiment was performed to validate the neutron spectrum inversion process. This additional exposure was a blind experiment in that the switchyard moderators were changed by LANSCE personnel to alter the incident neutron shape in a manner unknown to us and the uranium foil fission chamber was disconnected from the data collection system. We collected an energy deposition spectrum as before and used the inversion process from Eq. (3) to give a measurement of the incident neutron spectrum. Figure 7 shows this inverted spectrum, which agrees with the spectrum calculated by LANSCE using software for beam-shaping applications. Some systematic error is observed in this figure; the inverted neutron spectrum is consistently lower than the modeled spectrum below about 80 MeV and higher than the model above about 200 MeV. The systematic error is less than 30%; the systematic error may be due to the computer code, the inversion process, or both. Further investigations are under way to address the source of the systematic error.

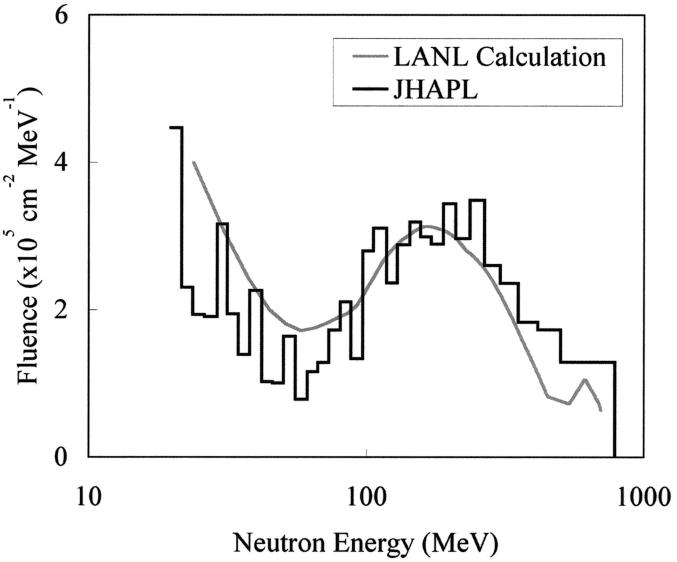

FIG. 7. Comparison of measured differential neutron fluence using the silicon detector and the response function inversion process with the calculated neutron fluence from LANSCE beam-shaping software for the validation experiment.

Application to Shielding Study

As part of our August 2000 experiments, we measured the change in neutron spectrum through polyethylene slabs of thickness from 5 to 15 cm. Figure 4 shows the experimental configuration, including the position of the polyethylene slabs in the LANSCE beamline. The purpose of these measurements was to study the effectiveness of polyethylene for high-energy neutron shielding and to assess the usefulness of the silicon detector system for practical neutron spectrum measurement.

High-energy neutrons interact with polyethylene mainly through elastic collisions with hydrogen nuclei. The products of the elastic collisions are protons and neutrons of lower energy than the incident neutron. Secondary protons passing through the detector in our experimental configuration were detected with near 100% efficiency, while neutrons were detected with an efficiency of a few percent (Fig. 1) as were neutrons from the primary beam that did not interact with the polyethylene; depositions in our detector were due to both protons and neutrons. We used simulations from MCNPX (*10*) to estimate the deposition spectra for the proton component and subtracted these from the overall measured deposition spectra. The corrected spectra were inverted using the technique discussed above to estimate neutron spectra after passage through the polyethylene slabs.

Figure 8 gives the integral neutron spectra behind each polyethylene shield. Figure 9 shows the resulting integral ($>$20 MeV) flux as a function of polyethylene thickness. These data indicate that for environments that contain high-energy neutrons such as the International Space Station, at least 10 cm of polyethylene shielding is needed to significantly reduce neutron flux above 20 MeV. Adding addi-

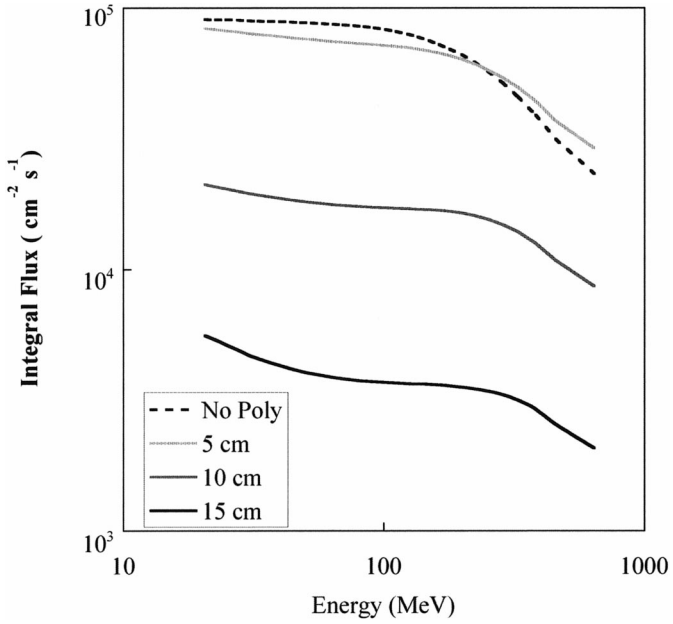

FIG. 8. Integral neutron flux spectra for each polyethylene slab in the shielding experiment, along with the unshielded beam for comparison. The calculated secondary proton flux has been subtracted from the total shielded deposition spectra prior to the inversion process that deduces the neutron spectra.

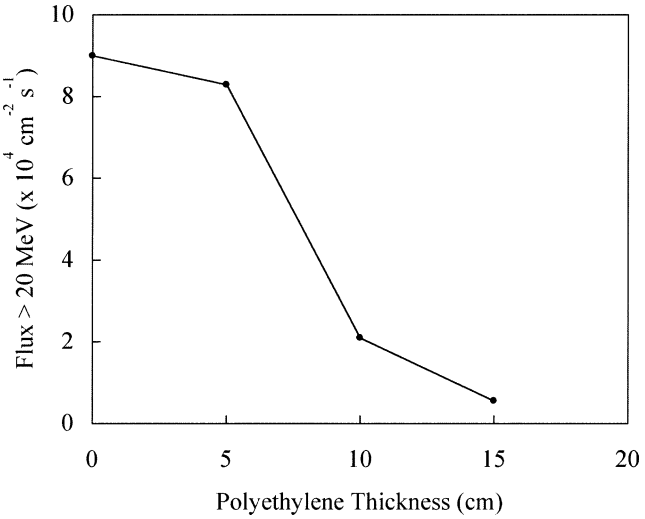

FIG. 9. Integral neutron flux (>20 MeV) from thick silicon detector measurements as a function of shield thickness after correction for secondary proton generation in polyethylene.

tional shielding decreases the neutron flux further, but at ever decreasing effectiveness. Future experiments are planned to examine the high-energy neutron shielding properties of other materials commonly used in manned spacecraft and in planetary structures built from local regolith. These future experiments will incorporate charged-particle discrimination to eliminate the need to correct for charged secondaries produced along with neutrons in shielding interactions and will extend the neutron spectra to lower energies.

SUMMARY

We have demonstrated that thick silicon detectors can be used to measure neutron spectra over an energy range of 20–800 MeV. The measurement technique is reasonably efficient and can be implemented in a small volume. The detector system described here forms the high-energy channel of a neutron spectrometer flown on several high-altitude aircraft flights, and it is included in a suite of sensors soon to be flown on a long-duration balloon flight to measure the neutron spectrum at atmospheric depths similar to that found on the surface of Mars and to the shielding depth surrounding astronauts in the International Space Station. The balloon flight instrument will be a precursor for instrument concepts to be proposed as an instrument for space flight environmental measurements.

In addition, we are developing a detailed model of the detector response to neutrons using high-energy physics tools which incorporate fundamental physical models of neutron interactions with nuclei. This model will be used to further validate the use of thick silicon detectors for neutron spectroscopy and to optimize the performance of the detector in a mixed radiation field when combined with anti-coincidence shielding and to guide further experiments in neutron spectroscopy with silicon detectors. The model will also be used to guide the design of further shielding experiments.

ACKNOWLEDGMENTS

This work was supported by the National Aeronautics and Space Administration through NASA Cooperative Agreement 9-58 with the National Space Biomedical Research Institute and NASA Research Grant NAG8-1695 with Marshall Space Flight Center.

Received: February 13, 2002; accepted: September 4, 2002

REFERENCES

1. G. D. Badhwar, J. E. Keith and T. F. Cleghorn, Neutron measurements on board the Space Shuttle. *Radiat. Meas.* **33**, 235–241 (2001).
2. E. Normand and T. J. Baker, Altitude and latitude variations in avionics SEU and atmospheric neutron flux. *Trans. Nucl. Sci.* **40**, 1484 (1993).
3. J. W. Wilson, L. W. Townsend, W. Schimmerling, G. S. Khandelwal, F. Khan, J. E. Nealy, F. A. Cucinotta, L. C. Simonsen, J. L. Shinn and J. W. Norbury, *Transport Methods and Interactions for Space Radiation.* NASA Reference Publication 1257. NASA Scientific and Technical Information Program, Washington, DC, 1991.
4. M. B. Chadwick, P. G. Young, S. Chiba, S. C. Frankle, G. M. Hale, H. G. Hughes, A. J. Koning, R. C. Little, R. E. MacFarlane and L. S. Waters, Cross-section evaluations to 150 MeV for accelerator-driven systems and implementation in MCNPX. *Nucl. Sci. Eng.* **131**, 293–328 (1999).
5. G. F. Knoll, *Radiation Detection and Measurement.* Wiley, New York, 2000.
6. W. E. Burcham, *Nuclear Physics.* Longman Group, London, 1973.
7. C. L. Lawson and R. J. Hanson, *Solving Least Squares Problems.* Prentice-Hall, New York, 1974.

8. P. W. Lisowski, C. D. Bowman, G. J. Russell and S. A. Wender, The Los Alamos National Laboratory spallation neutron sources. *Nucl. Sci. Eng.* **106**, 208 (1990).

9. S. A. Wender, S. Balestrini, A. Brown, R. C. Haight, C. M. Laymon, T. M. Lee, P. W. Lisowski, W. McCorkle, R. O. Nelson and N. W. Hill, A fission ionization detector for neutron flux measurements at a spallation source. *Nucl. Instrum. Methods Phys. Res.* **A336**, 226 (1993).

10. L. S. Waters, Ed., *MCNPX Users Manual.* Technical Report TPO-E83-G-UG-X-00001, Los Alamos National Laboratory, Los Alamos, NM, 1999.